

Research Paper

Cite this article: Zafar S, Nawaz MI, Aras E, Tendurus G, Urfali E, Kashif A, Ozbay E (2025) Design of a sub-1.4 dB noise figure robust X-band LNA using GaN HEMT technology. *International Journal of Microwave and Wireless Technologies*, 1–9. <https://doi.org/10.1017/S1759078725102304>



Received: 2 May 2025
Revised: 23 August 2025
Accepted: 4 September 2025

Keywords:

GaN-on-SiC; inductive source degeneration; low-noise amplifier; reverse recovery time; survivability

Corresponding author: Salahuddin Zafar;
Email: zafar@ee.bilkent.edu.tr

Design of a sub-1.4 dB noise figure robust X-band LNA using GaN HEMT technology

Salahuddin Zafar¹ , Muhammad Imran Nawaz^{1,2} , Erdem Aras^{1,2},
Gizem Tendurus¹, Emirhan Urfali¹, Ahsanullah Kashif³ and Ekmel Ozbay^{1,2,4}

¹Nanotechnology Research Center, Bilkent University, Ankara, Turkey; ²Department of Electrical and Electronics Engineering, Bilkent University, Ankara, Turkey; ³Department of Electrical Engineering, IIUI, Islamabad, Pakistan and ⁴Department of Physics, Bilkent University, Ankara, Turkey

Abstract

Gallium nitride technology takes advantage of the survivability for low-noise applications, while SiGe and GaAs technologies are recognized for the better noise figure (NF). In this paper, the technique for implementing inductive source degenerated HEMTs in all the stages to have a better NF is combined with a technique of high value gate bias resistor (R_{GB}) to improve survivability. Moreover, this work includes the dependence of the reverse recovery time on different values of R_{GB} with respect to the trap phenomenon and the RC time constant. The designed low-noise amplifier (LNA) achieves an NF better than 1.4 dB for 7.5–11.5 GHz, OIP3 up to 33 dBm, input reflection coefficient better than -8.4 dB, and output reflection coefficient better than -11.1 dB. NF has a minimum of 1.15 dB at 9.9 GHz. The small-signal gain of LNA is better than 15.3 dB in the whole frequency band, and the output power at 1 dB gain compression is 23 dBm at 11.5 GHz. LNA survives an input stress level of up to 39 dBm. The dimensions of the designed LNA MMIC are 2.9 mm \times 1.3 mm.

Introduction

Gallium nitride (GaN) technology has outperformed competitive technologies such as GaAs, SiGe, BiCMOS, and CMOS for power applications. GaN technology has also proved useful in low-noise applications due to built-in power handling capability, high linearity, and compact transceiver designs [1–3]. A 60 nm GaN-on-Si process has shown better noise results up to 10 GHz at the device level compared to a 70 nm GaAs counterpart [4].

Survivability and noise figure (NF) are two of the most important figures of merit (FoMs) for a low-noise amplifier (LNA) design. There have been reports of highly survivable and low NF X-band GaN LNA monolithic microwave integrated circuits (MMICs). More than 37 dBm survivability has been reported in [5–8] with an NF of better than 2 dB in all these designs. On the other hand, sub-1.8 dB NF LNA designs have been reported based on 0.09 and 0.25 μ m GaN technology [9–13]. A high value gate bias resistor (R_{GB}) technique was employed to achieve 42 dBm survivability [3]. In another work, sub-1.2 dB NF was achieved owing to the choice of inductive source degenerated (ISD) HEMTs at both stages [14].

In the proposed work, the above-mentioned techniques, R_{GB} and ISD at both stages, have been combined to achieve a low NF and robust LNA. Another focus of this work is bandwidth enhancement to report a 7.5–11.5 GHz broadband LNA. Along with other promising small-signal results, achieved sub-1.4 dB NF combined with 39 dBm survivability for 7.5–11.5 GHz is the best reported for GaN technology to date, to the best of the authors' knowledge.

Reverse recovery time (RRT), a critical FoM for an LNA, refers to the time required for the gate bias to retrieve its steady-state value after the removal of an input stress. RRT depends primarily on the RC time constant and the trap phenomenon [3]. The RC time constant is determined by R_{GB} , gate bias capacitors (blocking and bypass capacitors), and the HEMT's input capacitance (C_{in}). On the other hand, the trap phenomenon is inherent to the properties and fabrication processes of the GaN material. In [3], it is shown that the trap phenomenon is a major contributor to RRT after a particular level of input stress. This work experimentally shows that for a fixed value of input stress, where the traps are already excited, RRT is not a linear function of the RC time delay with changing value of R_{GB} . This is a critical study in choosing R_{GB} to address LNA's robustness, especially for radar applications.

The fabrication process of the device and MMIC is discussed in the second section, while the HEMT parameters and LNA design are discussed in section "LNA design". "Results and

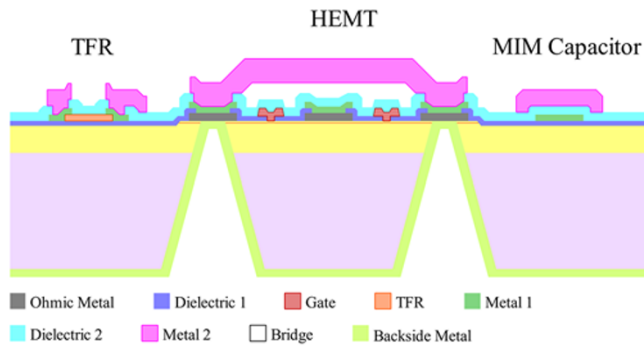


Figure 1. Sketch of NANOTAM's fabrication process [15].

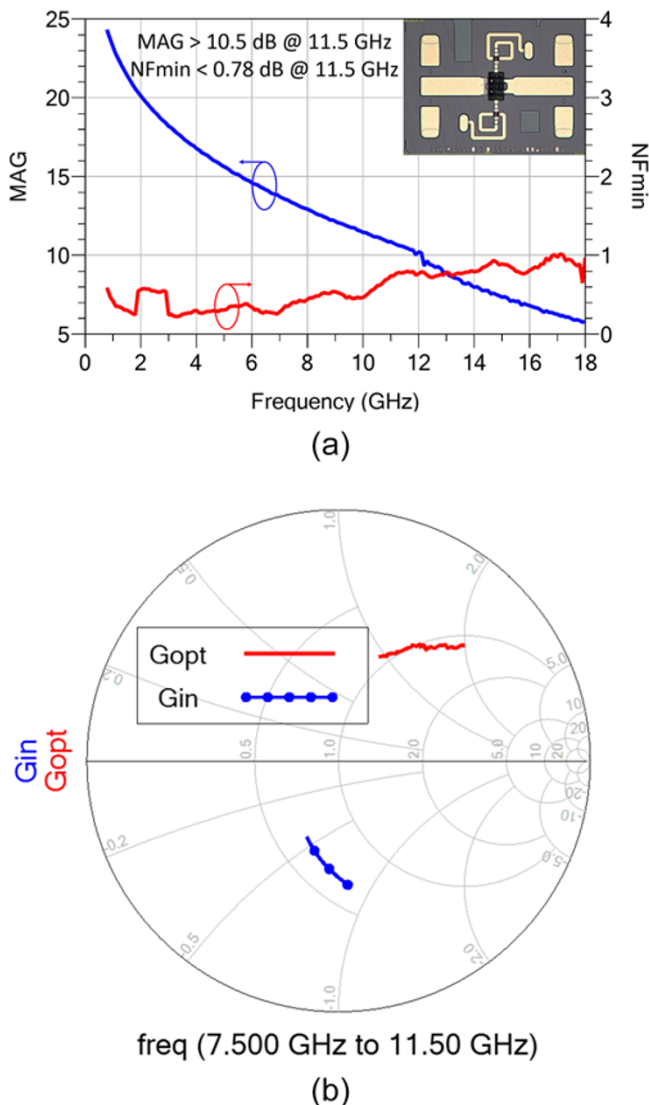


Figure 2. (a) MAG and NF_{min} ; (b) Γ_{opt} and Γ_{in} of $4 \times 75 \mu m$ ISD HEMT, denoted by G_{opt} and G_{in} , respectively, for 12 V, 200 mA/mm.

discussions" section covers the measured results of the fabricated MMIC, including small-signal, large-signal, survivability, and RRT. The conclusion is drawn in the last section.

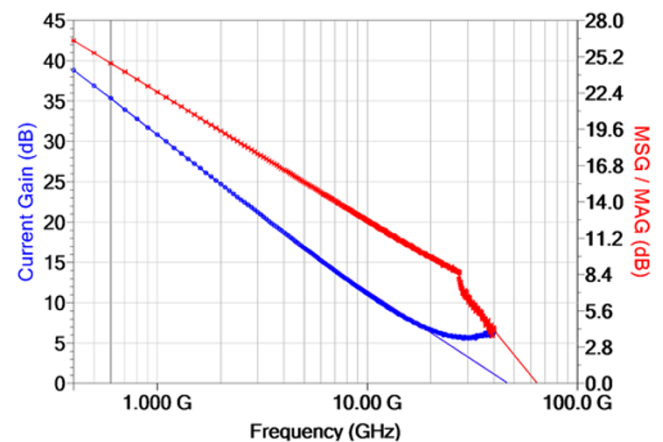


Figure 3. f_T and f_{max} of $4 \times 75 \mu m$ HEMT as extrapolation curves for current gain and MAG.

Fabrication process

NANOTAM's $0.15 \mu m$ AlGaIn/GaN on SiC fabrication process is used for low-noise applications in the X-band. The epitaxial structure of HEMT, grown on a 3-inch SiC substrate by metal-organic chemical vapor deposition, consists of AlN nucleation, Fe-doped GaN buffer, GaN transition and channel layers, AlGaIn barrier layer, and GaN cap layer. The next step is the fabrication of active and passive devices over the grown wafers. Ohmic contact formation (120 nm Ti/Al/Ni/Au stack), mesa isolation etching, a dielectric passivation layer, and gate formation (Ni/Au stack with 500 nm gate head and 150 nm gate foot) are related to active device fabrication. Mesa-etched regions are also used as high value resistances that have a density of $250 \Omega/\square$. Passive device fabrication includes 80 nm TaN deposition to realize $30 \Omega/\square$ thin-film resistor (TFR). It also includes metal-insulator-metal (MIM) capacitor formation with 220 nm thick dielectric layer of Si_xN_y giving on-chip $270 pF/mm^2$ capacitance density. Backside process, the last step of fabrication, involves backside thinning of $100 \mu m$, back-via holes opening through SiC substrate, and Au layer coating of $5.5 \mu m$ thickness. The back-vias serve the purpose of ground connections for microstrip transistors and circuits. Figure 1 shows the final sketch of the wafer, including active device and passive components.

LNA design

HEMT's selection and characterization

The first and foremost step in designing an LNA is the choice of a suitable HEMT. The deciding factors in this choice include the periphery and topology of HEMT. The choice of the periphery of the HEMT depends upon the maximum available gain (MAG) and minimum noise figure (NF_{min}). In our two-stage LNA design, we have chosen $4 \times 75 \mu m$ ISD HEMT for both stages. The reason for choosing this periphery includes its MAG value of >10.5 dB and promising NF_{min} value of <0.78 dB in the frequency band of interest from 7.5 to 11.5 GHz, as evident from Figure 2a. The parallel step is the topology selection, ISD or common source (CS). Compared to CS topology, ISD HEMTs have optimum noise impedance (Γ_{opt}) as the conjugate of input impedance (Γ_{in}), allowing the LNA designer to match the input reflection coefficient (IRC) and NF simultaneously [14]. Figure 2b shows Γ_{opt} and Γ_{in}

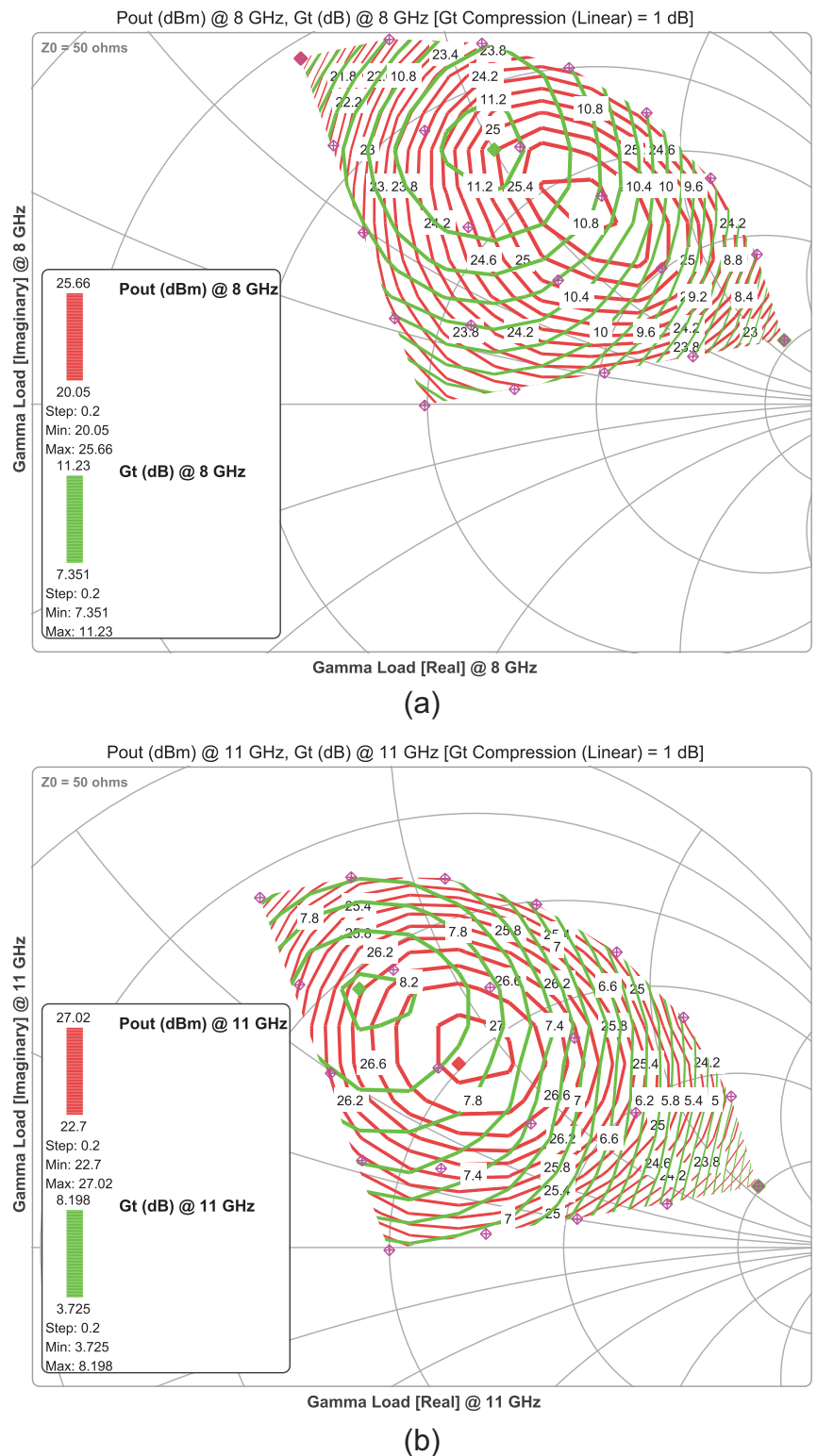


Figure 4. Load pull contours for $4 \times 75 \mu\text{m}$ ISD HEMTs at (a) 8 GHz; (b) 11 GHz for 12 V, 200 mA/mm.

of the selected $4 \times 75 \mu\text{m}$ ISD HEMT, denoted by G_{opt} and G_{in} , respectively. An added advantage of ISD implementation in HEMT is avoiding the resistive network for stabilization towards the gate side, thus keeping NF at a low value [14]. Figure 3 shows f_T and f_{max} of $4 \times 75 \mu\text{m}$ HEMT determined to be 46.5 and 63.9 GHz by extrapolating the current gain and MAG, respectively.

Figure 4a and 4b show load pull measurements of $4 \times 75 \mu\text{m}$ ISD HEMT at 8 and 11 GHz respectively. The closeness of optimum impedance points for power and gain from load and gain circles leads to the option of the simultaneous match for output power and output reflection coefficient (ORC).

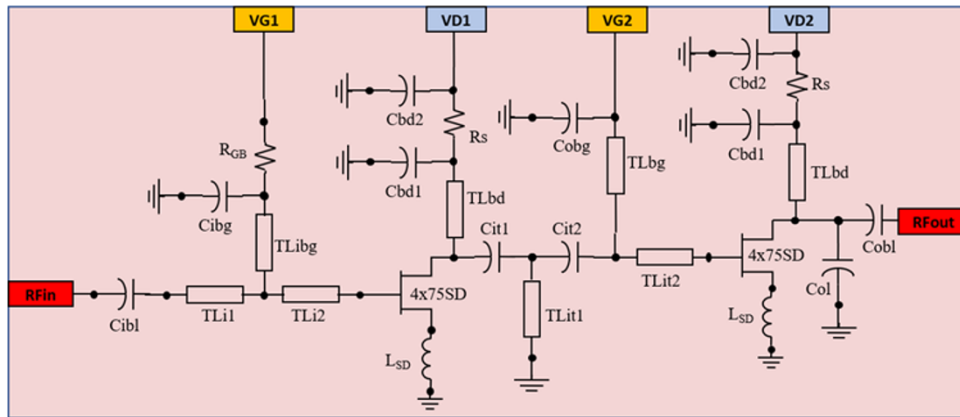


Figure 5. Schematic diagram of the proposed LNA.

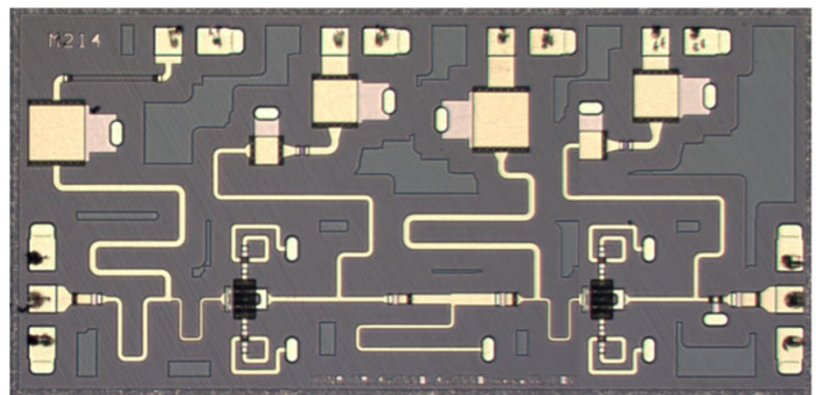


Figure 6. Microphotograph of the fabricated LNA.

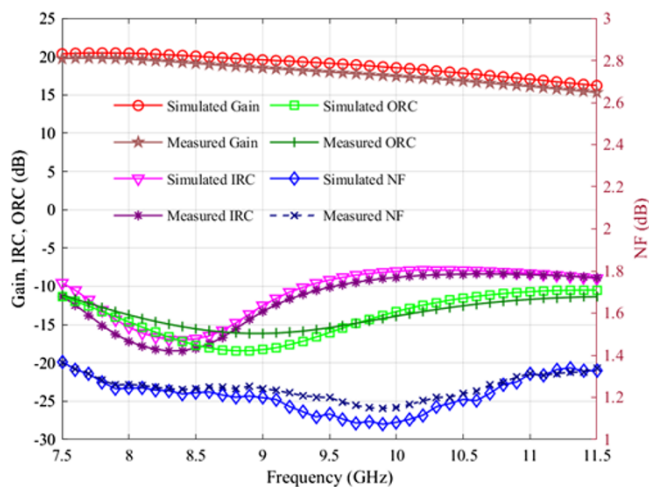


Figure 7. Simulated and measured small-signal gain, reflection coefficients, and NF.

MMIC design and simulations

Figure 5 shows the schematic diagram of the proposed LNA, and Figure 6 shows the microphotograph of the fabricated LNA MMIC having the dimensions of 2.9 mm \times 1.3 mm. The design starts with the stabilization of HEMTs, where the first stage HEMT is stabilized for frequencies greater than 2 GHz using $TLbd$, R_s , $Cbd1$, and $Cbd2$. For lower frequencies, stability is ensured by $TLi2$,

$TLbg$, and $Cibg$. Second-stage HEMT is stabilized by adopting a similar procedure. As mentioned in Section “HEMT’s selection and characterization,” no resistive component is used towards the gate side of the HEMT, ensuring a low NF in the final design. Although the contribution of noise from the second stage, according to the Friis formula, is small, it has the role of deciding the final NF of a multi-stage LNA [14].

After fulfilling the unconditional stability condition, the design continues with input, inter-stage, and output matching networks. The stability networks further serve the purpose of gate and drain bias as well as matching, leading to a compact design. $TLi1$ and $Cibl$ complete the input matching network, while Col and $Cobl$ are further components for output matching network. Inter-stage matching network is finalized with $Cit1$, $Cit2$, and $TLit1$. L_{SD} connected to the source terminal of HEMT represents the source degeneration. Finally, R_{GB} is 5 k Ω mesa resistor in the gate bias line of the first stage to amplify the survivability of LNA. The scope of the design of this paper includes small and large-signal measurements, as well as robustness. Measurements are focused on small-signal, noise, output power at 1-dB compression point (OP_{1dB}), output third-order intercept point ($OIP3$), survivability, and RRT.

Electromagnetic (EM) simulations are accomplished using PathWave Advanced Design System (ADS) from Keysight Technologies.¹ All matching networks are optimized simultaneously due to their effect on each other because small periphery HEMTs have little reverse isolation. Figure 7 shows that EM simulations result in small-signal gain >16.2 dB, NF <1.37 dB,

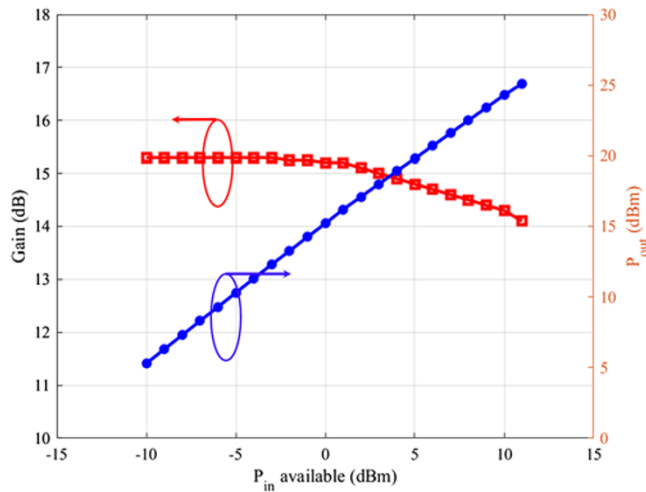


Figure 8. OP_{1dB} of fabricated MMIC at 11.5 GHz.

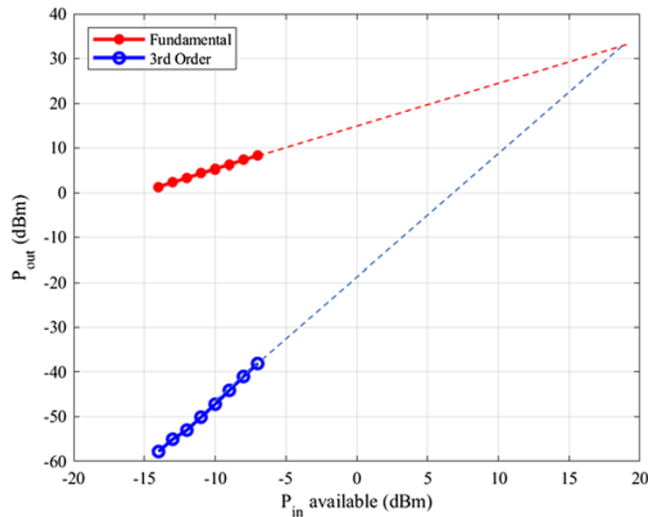


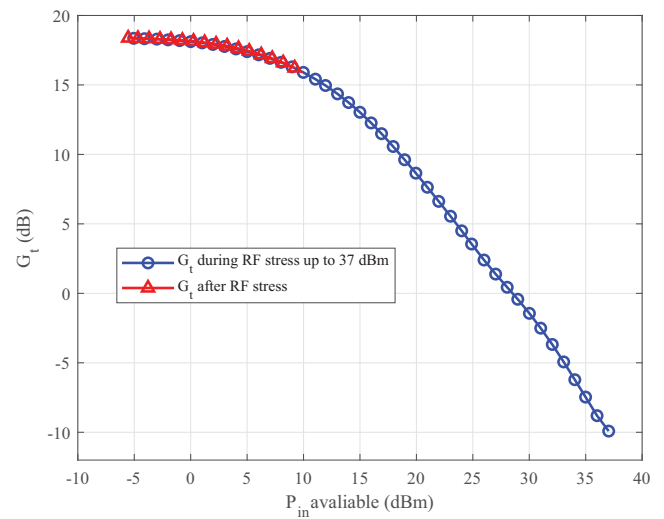
Figure 9. OIP_3 of fabricated MMIC for 12 V, 200 mA/mm.

$IRC < -8$ dB, and $ORC < -10.5$ dB in the desired frequency band.

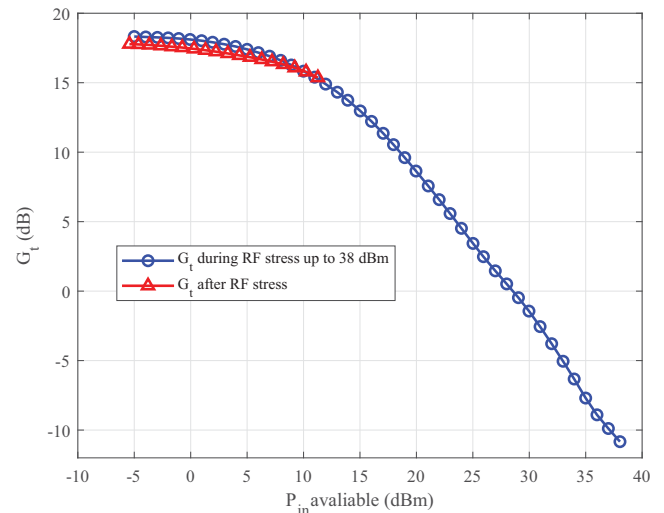
Results and discussions

Small-signal and noise measurements are carried out using PNA-X from Keysight Technologies, ZVA40 from Rohde & Schwarz,² and DC & RF probes from the GGB industries.³ Maury's⁴ tuners, FormFactor's⁵ probe station, and IVCAD software of Amcad Engineering⁶ are utilized for large-signal measurements. We used the DSOS204A oscilloscope and the E8257D pulsed signal generator from Keysight Technologies for the recovery time measurements.

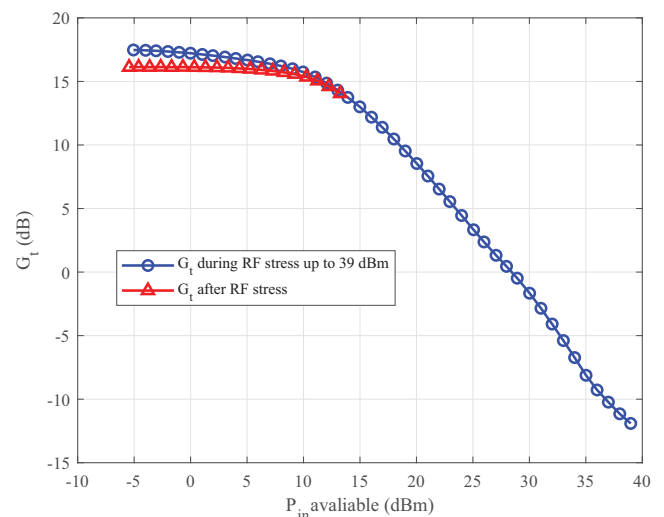
The bias condition for all the measurements is 12 V, 200 mA/mm under the base temperature of 25 °C. The small-signal, noise, and linearity measurements are performed with continuous wave (CW) signals, while survivability measurements are performed under pulse conditions having a 250 μ s pulse period and 25 μ s pulse width.



(a)



(b)



(c)

Figure 10. Gain before and after input stress levels of (a) 37, (b) 38, and (c) 39 dBm at 10 GHz.

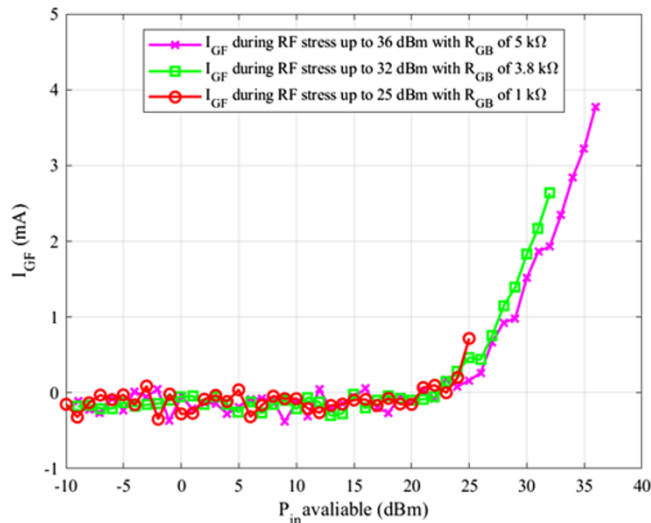


Figure 11. Variation in I_{GF} with change in the value of R_{GB} .

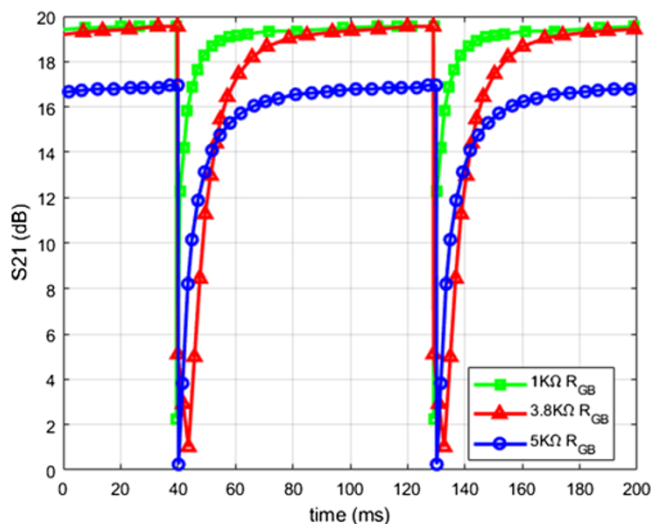


Figure 12. RRT for $P_{in} = 25$ dBm and R_{GB} values of 1, 3.8, and 5 kΩ.

Small-signal and noise results

Figure 7 demonstrates the small-signal and noise characteristics of the fabricated MMIC. Small-signal gain greater than 15.3 dB and NF less than 1.36 dB are achieved for the bandwidth 7.5–11.5 GHz. A minimum NF of 1.15 dB is measured at 9.9 GHz. IRC and ORC are less than -8.4 and -11.1 dB, respectively, in the whole frequency band of interest. The measured and simulation results are in close agreement with each other. The promising values of NF and IRC at the same time are indicators of the advantage of ISD implementation in HEMT, as discussed in Section “HEMT’s selection and characterization.”

The value of obtained NF depends on the matching of the optimum noise impedance values and the resistive losses of the matching networks. To obtain the broadband response of NF across the 4 GHz bandwidth, the matched impedance values may slightly differ from the optimum values, which leads to a difference between NF_{min} of HEMT and the obtained NF of LNA. Moreover, as explained in Section “HEMT’s selection and characterization,” although the ISD HEMT topology keeps NF at a low value by

avoiding the resistive network towards the gate side for stability, there is still a resistive contribution due to lossy components of the matching networks mentioned in Section “MMIC design and simulations” for the stability of both stages. This is another reason for the deviation of the NF_{min} and the NF value. Furthermore, according to the Friis equation, although small, there is a contribution to the overall NF of the LNA from the second stage. In the proposed LNA, we have achieved an NF of less than 1.4 dB in the entire frequency band of interest compared to the individual HEMT having an NF_{min} of <0.78 dB from 7.5 to 11.5 GHz.

Large-signal and survivability measurements

OP_{1dB} and $OIP3$ values, indicators of the linearity, are measured to be 23 and 33 dBm, respectively, at 11.5 GHz, as evident from Figure 8 and 9. Survivability is a measure of the ability of an LNA in the receive chain to handle high input power levels. LNA is subjected to input stress levels of 37, 38, and 39 dBm in steps at 10 GHz, and small-signal gain is measured after each step, as shown in Figure 10a–c, respectively. LNA survives an input stress level up to 39 dBm without significant degradation in the gain.

Recovery time measurements

For RRT analysis using different values of R_{GB} , LNA design from our previously published work [3] with the new fabrication is used. RRT is a function of the RC time constant and the trap phenomenon. As explained in [3], traps are excited after a particular input stress level, after which RRT becomes a dominant phenomenon and a major contributor to recovery time. Figure 11 depicts the variation of the forward gate current I_{GF} with increasing input stress level for different values of R_{GB} . As expected, it is evident that the value of I_{GF} , an indicator of trap excitation, at 25 dBm input power (P_{in}) level is almost similar for R_{GB} values of 1, 3.8, and 5 kΩ. Therefore, $P_{in} = 25$ dBm is a reasonable choice to observe the behavior of R_{GB} value towards RRT for the same level of trap excitation.

RRT for an input stress level of 25 dBm and R_{GB} values of 1, 3.8, and 5 kΩ is measured to be 60, 80, and >90 ms, respectively, as shown in Figure 12. The pulse conditions for the RRT measurements are 200 μ s pulse width and 90 ms pulse period. It is evident that the LNA recovers fully for R_{GB} values of 1 and 3.8 kΩ during the pulse relaxation time, while full recovery is not achieved for R_{GB} value of 5 kΩ. This is the reason that the gain for 5 kΩ R_{GB} LNA never touches its initial small-signal gain value of ~ 20 dB.

The values of the DC block capacitor, bypass capacitor, and C_{in} are 0.4, 10, and 0.3 pF, respectively. RC time delay of 1, 3.8, and 5 kΩ R_{GB} for 10% to 90% is calculated to be 23.5, 89.5, and 117.7 ns. It shows that RRT is not linearly dependent on the RC time constant with increasing values of R_{GB} . It is experimentally concluded that the gate shifted to the negative value with increasing R_{GB} takes much more time to return to its normal value than the expected RC time constant. Hence, after the trap excitation due to high input stress, RRT becomes a non-linear function of R_{GB} .

It is worth mentioning that the use of an R_{GB} of even greater value can enhance the ability of LNA to restrict the I_{GF} , but at the cost of the shift in the gate bias voltage. Moreover, the factor that limits the choice of higher R_{GB} is the ability of HEMT to withstand the negative voltage peak value before the breakdown [15].

Table 1. A comparison of designed MMIC with the recently reported GaN-based and other competitive technologies at X-band

Reference	BW (GHz)	NF (dB)	Gain (dB)	IRC (dB)	ORC (dB)	OP _{1dB} /OIP3 (dBm)	P _{DC} (mW)	Size (mm ²)	FoM	Lg (μm)	Tech
This work	7.5–11.5	<1.4	>15.3	<-8.4	<-11.1	23/33	1440	3.77	14.3	0.15	GaN
[9]	9–11	<1.5	>13.5	<-10	<-8*	-/28-30	800	2.56	–	0.09	GaN
[10]	8–11	<1.6	>22.5	<-10	<-8	12/24	500	2.73	12	0.25	GaN
[11] LNA A	8–10	<1.3	>24	<-2	<-12.5	21*/33.8	900	4.5	27	0.25	GaN
[11] LNA B	10–12	<1.75	>24.4	<-10	<-12	21*/32.8	900	4.5	23	0.25	GaN
[12]	7.4–11.4	<1.6	>23	<-10	<-10	22.5/-	1200	6.06	29	0.25	GaN
[13]	8–12	<1.8	>14	–	–	-/19.5	210	6	–	0.25	GaN
[14] LNA-1	8–11	<1.2	>16.8	<-10.3	<-10.1	21/31-34	1440	3.7	12.4	0.15	GaN
[14] LNA-2	8–11	<1.7	>17.2	<-11.6	<-9.2	17/27-30	1440	3.7	1.6	0.15	GaN
[16]	6.5–10	<1.6*	>15	–	–	–	–	6	–	0.25	GaN
[17]**	7–10	<2.1	>24	<-10	<-18	7-13/-	540	2.3	2.7	0.25	GaN
[18]	8–12	<2	>20	<-13	<-13	15-25/-	810/1710	–	22	0.10	GaN
[19]	9–10	<1.6	>18.7	<-10	<-11.5	20.5/-	930	4.4	6.5	0.25	GaN
[20]	8–10	<1.4	>25	<-8	<-8	0.5/-	190	3.6	0.76	0.15	GaAs
[21]	10.7–13.1	<1.7*	>17*	<-8*	<-8*	–	42.4	2	–	0.15	GaAs
[22]	8–12	<1.8	>24	<-15	–	10/-	175	7.68	21	–	GaAs
[23]	8–12	<1.5**	>19.6	<-13	<-14	13**/-	215	2.64	18.3	0.25	GaAs
[24]	8–10	<4.25	>14*	<-10	<-10	14-15/25.5-29.6	289.5	1.5	-8.7	0.25	GaAs
[25]	8–12	<1.6*	>18*	<-10*	<-10*	18.75/24.75	100.8	0.72	32.5	0.13	SiGe
[26]	6.4–11	<1.3*	>21*	<-6*	<-2*	2.5/-	32.8	0.46	20.3	0.18	SiGe
[27]	8–12	<1.4	>25*	<-10*	<-10*	13.8/40	10.44	0.437	57.7	0.065	CMOS

*Estimated values from figures; **Simulation-based values.

Comparison

Table 1 summarizes the state-of-the-art LNAs based on GaN and other competitive technologies with sub-1.8 dB NF, including this work. FoM is based on small-signal gain, OP_{1dB}, bandwidth (BW), NF, P_{DC}, and the center frequency (f_o) as follows [28]:

$$FoM = 20 \log_{10} \left(\frac{Gain [abs] \cdot OP_{1dB} [mW] \cdot BW [GHz]}{(NF [abs] - 1) \cdot P_{DC} [mW] \cdot f_o [GHz]} \right) \quad (1)$$

This work reports competitive performance compared to GaN-based designs in the similar frequency band and with CMOS, GaAs, and SiGe technologies.

Conclusion

An X-band GaN-based LNA MMIC is fabricated using NANOTAM's 0.15 μm technology. The advantages of ISD HEMTs in terms of easy stabilization to maintain low NF_{min} and simultaneous match condition for noise and IRC are exploited to design a two-stage LNA with a promising NF value of less than 1.4 dB. This NF value is close not only to the reported GaN-based designs but also to the SiGe and GaAs technologies recognized for the best noise performance. Along with achieving sub-1.4 dB NF for the frequency band of 7.5–11.5 GHz, LNA exhibits promising small-signal and linearity results. The design also covers the aspect of robustness by implementing high value R_{GB}, acting as a limiter to survive high power levels up to 39 dBm. Recovery time

measurements and their dependence on the different values of R_{GB} are also analyzed in this work. It is concluded that after trap excitation due to high input stress, RRT becomes a non-linear function of R_{GB}.

Acknowledgements. The authors are obliged to NANOTAM's fabrication and measurement teams.

Competing interests. The authors declare none.

Notes

- ¹ Keysight Technologies, Inc., Santa Rosa, CA, USA.
- ² Rohde & Schwarz GmbH & Co. KG., München, Germany.
- ³ GGB Industries Inc., Naples, FL, USA.
- ⁴ Maury Microwave Technologies, Ontario, CA, USA.
- ⁵ FormFactor Inc., Livermore, CA, USA.
- ⁶ AMCAD Engineering, Limoges, France.

References

1. Rudolph M (2017) GaN HEMTs for low-Noise Amplification – Status and challenges. Integrated Nonlinear Microwave and Millimetre-Wave Circuits Workshop (INMMiC), 1–4, Graz, Austria, IEEE.
2. Schuh P, Sledzik H and Reber R (2018) GaN-based single-chip frontend for next-generation X-band AESA systems. *International Journal of Microwave and Wireless Technologies* **10**(5-6), 660–665.

3. Zafar S, Akoglu BC, Aras E, Yilmaz D, Nawaz MI, Kashif A and Ozbay E (2022) Design and robustness improvement of high-performance LNA using 0.15 μm GaN technology for X-band applications. *International Journal of Circuit Theory and Applications* 50(7), 2305–2319.
4. Ciccognani W, S Colangeli, A Serino, L Pace, S Fenu, PE Longhi, E Limiti, J Poulain and J Leblanc (2019) Comparative noise investigation of high-performance GaAs and GaN millimeter-wave monolithic technologies. 2019 14th European Microwave Integrated Circuits Conference (EuMIC), 192–195, Paris, France, IEEE.
5. Kim B and W Gao (2016) X-Band robust current-shared GaN low noise amplifier for receiver applications. IEEE Compound Semiconductor Integrated Circuits Symposium (CSICS), 1–4, Austin, TX, USA, IEEE.
6. Janssen JPB, M van Heijningen, G Provenzano, GC Visser, E Morvan and FE van Vliet (2008) X-band robust AlGaIn/GaN receiver MMICs with over 41 dBm power handling. 2008 IEEE Compound Semiconductor Integrated Circuits Symposium, 1–4, Monterey, CA, USA, IEEE.
7. Bettidi A, Corsaro F, Cetronio A, Nanni A, Peroni M and Romanini P (2009) X-Band GaN-HEMT LNA Performance Versus Robustness trade-off. 2009 European Microwave Conference (EuMC), 1792–1795, Rome, Italy, IEEE.
8. Micovic M, A Kurdoghlian, T Lee, RO Hiramoto, P Hashimoto, A Schmitz, I Milosavljevic, PJ Willadsen, WS Wong, M Antcliffe, M Wetzel, M Hu, MJ Delaney and DH Chow (2007) Robust broadband (4 GHz–16 GHz) GaN MMIC LNA. 2007 IEEE Compound Semiconductor Integrated Circuits Symposium, 1–4, Portland, OR, USA, IEEE.
9. Kobayashi KW, V Kumar, C Campbell, S Chen, Y Cao and J Jimenez (2020) Robust-5W reconfigurable S/X-band GaN LNA using a 90nm T-gate GaN HEMT technology. 2020 IEEE BiCMOS and Compound Semiconductor Integrated Circuits and Technology Symposium (BCICTS), 1–4, Monterey, CA, USA, IEEE.
10. Yağbasan C and A Aktuğ. (2018) Robust X-Band GaN LNA with integrated active limiter. 2018 48th European Microwave Conference (EuMC), 1205–1208, Madrid, Spain, IEEE.
11. Vittori M, S Colangeli, W Ciccognani, A Salvucci, G Polli and E Limiti (2017) High performance X-band LNAs using a 0.25 μm GaN technology. 13th Conference on Ph.D. Research in Microelectronics and Electronics (PRIME), Giardini, 157–160, Naxos-Taormina, Italy, IEEE.
12. D'Angelo S, A Biondi, F Scappaviva, D Resca and VA Monaco (2016) A GaN MMIC chipset suitable for integration in future X-band spaceborne radar T/R module Frontends. 2016 21st International Conference on Microwave, Radar and Wireless Communications (MIKON), 1–4, Krakow, Poland, IEEE.
13. Schuh P and R Reber (2013) Robust X-band low noise limiting amplifiers. 2013 IEEE MTT-S International Microwave Symposium Digest (MTT), 1–4, Seattle, WA, USA, IEEE.
14. Zafar S, Aras E, Akoglu BC, Tendurus G, Nawaz MI, Kashif A and Ozbay E (2022) Design of GaN-based X-band LNAs to achieve sub-1.2 dB noise figure. *International Journal of RF and Microwave Computer-Aided Engineering* 32(11), e23379.
15. Zafar S (2022) Design and development of X-band GaN-based low-noise amplifiers. *PhD Thesis*, Ankara, Turkey: Bilkent University.
16. Schuh P, Sledzik H and Reber R, Fleckenstein A, Leberer R, Oppermann M, Quay R, van Raay F, Seelmann-Eggebert M, Kiefer R and Mikulla M. (2009) X-band T/R-module front-end based on GaN MMICs. *International Journal of Microwave and Wireless Technologies* 1(4), 387–394
17. Yang S, Q Dong, W Huang, X Jiang, Y Wang and W Luo (2023) A Compact 7–10 GHz GaN Low Noise Amplifier MMIC with Sub 0.3 dB Gain flatness. 2023 IEEE 15th International Conference on ASIC (ASICON), 1–4, Nanjing, China, IEEE.
18. Pinault B, J-G Tartarin, D Saugnon and R Leblanc (2023) A self-reconfigurable highly linear and robust X-Band MMIC GaN LNA. 2023 18th European Microwave Integrated Circuits Conference (EuMIC), 13–16, Berlin, Germany, IEEE.
19. Saini E, S Sinha and PP Kumar (2024) High performance GaN LNA for space based radar front-end. 2024 IEEE Microwaves, Antennas, and Propagation Conference (MAPCON), 1–4, Hyderabad, India, IEEE.
20. Xie C, Yu Z and Tan C (2020) An X/Ku dual-band switch-free reconfigurable GaAs LNA MMIC based on coupled line. *IEEE Access* 8, 160070–160077.
21. Wang C, K-Y Chen, Y-L Lee and C-H Li (2019) A X — /Ku-band QFN-packaged GaAs LNA supporting dual-polarization signal reception. 2019 IEEE Asia-Pacific Microwave Conference (APMC), Singapore, 1521–1523, IEEE.
22. Zhou X, Y Li, G Zhou, H Wei, X Gao and H Wu (2018) Design of X-band miniature balanced limiter-low noise amplifier chip. 2018 International Conference on Microwave and Millimeter Wave Technology (ICMMT), 1–3, Chengdu, China, IEEE.
23. Jiang Y, G-D Su, D Sun, Y Huang, Z Lin and J Liu (2022) GaAs based MMIC LNA for X-band applications. 2022 IEEE MTT-S International Microwave Workshop Series on Advanced Materials and Processes for RF and THz Applications (IMWS-AMP), 1–3, Guangzhou, China, IEEE.
24. Bai X, Wu Y, Zhen S, Gao Z and Wang W (2025) A 8–10 GHz compact low noise amplifier MMIC with high linearity based on GaAs technology. *Microelectronics Journal* 162, 106742.
25. Davulcu M, I Kalyoncu and Y Gurbuz (2018) An X-Band SiGe BiCMOS triple-cascode LNA with boosted gain and $P_{1\text{dB}}$. *IEEE Transactions on Circuits and Systems II: Express Briefs* 65(8), 994–998.
26. Kanar T and Rebeiz GM (2014) X- and K-band SiGe HBT LNAs With 1.2- and 2.2-dB mean noise figures. *IEEE Transactions on Microwave Theory and Techniques* 62(10), 2381–2389.
27. RV, Gorre P, Song H and Kumar S (2021) Highly robust X-band quasi circulator-integrated low-noise amplifier for high survivability of radio frequency front-end systems. *International Journal of Circuit Theory and Applications* 49(7), 2170–2182.
28. Xuan X, Cheng Z, Gong T, Zhang Z and Le C (2024) An ultra-wideband current-reused LNA MMIC with negative feedback and adaptive bias networks. *International Journal of Microwave and Wireless Technologies* 16, (9), 1617–1622.



of AlGaIn/GaN on SiC-based MMICs.



His current research interests include the design and characterization of sub-system modules for RF and microwave frequencies and the development of AlGaIn/GaN on SiC-based MMIC amplifiers.

Salahuddin Zafar received MS degree in Electrical Engineering from NUST Islamabad, Pakistan, and PhD degree in Electrical and Electronics engineering from Bilkent University, Ankara, Türkiye, in 2012 and 2023, respectively. He has been working as a Senior Design Engineer in CESAT, Islamabad, and NANOTAM, Bilkent University, Ankara. His current research interests include the design and characterization of amplifiers for RF and microwave frequencies and the development

Muhammad Imran Nawaz received his BS degree in Electrical Engineering from NUST, Islamabad, Pakistan, in 2005. He completed his MS degree in Electromagnetic Field and Microwave Technology from NPU, Xi'an, China, in 2014, and his PhD in Electrical and Electronics Engineering from Bilkent University, Ankara, Türkiye, in 2025. He has been working as a Design Engineer in CESAT, Islamabad, and the Nanotechnology Research Center (NANOTAM), Bilkent University, Ankara.



Erdem Aras received the BS and MS degrees in Electrical and Electronics Engineering from Bilkent University, Ankara, Türkiye, in 2017 and 2020, respectively. He is currently pursuing his PhD degree in the same department. His doctoral research focuses on radio frequency (RF) and microwave monolithic integrated circuit (MMIC) design, with an emphasis on high-efficiency, low-noise, and high-power amplifier architectures. He

is also with the Nanotechnology Research Center (NANOTAM), where he works as an RF Design Engineer. At NANOTAM, he has been involved in the development of gallium nitride (GaN) on silicon carbide (SiC) high-electron-mobility transistor (HEMT) technologies operating up to 40 GHz. His research interests include high-power MMIC design, nonlinear device modeling, and thermal and electrical performance enhancement techniques in GaN HEMTs.



Gizem Tendurus received her BS and MS degrees in Electrical and Electronics Engineering from Başkent University, Ankara, Türkiye, in 2017 and 2022, respectively. She has been working as a senior RF Design and Application Engineer at Nanotechnology Research Center (NANOTAM), Ankara. Her expertise covers process characterization in S, C, X, and Ku band technologies, including DC, small-signal, large-signal, and noise measurements. Her design experience includes amplifier

MMIC development with a strong focus on phase shifters, switches, and low-noise amplifiers. She has also been actively involved in designing, testing, and packaging of GaN HEMTs specifically designed for radar and electronic warfare applications. With a solid foundation in both circuit design and measurement systems, she offers a comprehensive approach to high-performance RF and analysis.



Emirhan Urfali completed his BS in Electrical and Electronics Engineering from Başkent University, Ankara, Türkiye in 2019, and has since worked as an RF design engineer at NANOTAM, Ankara. His expertise covers process characterization across S-, C-, X-, and Ku-band, which includes DC, small-signal, large-signal, and noise measurements. His design experience includes amplifier MMIC development using cluster matching techniques, with a strong focus on stability and large-signal analysis.

He has also been involved in designing, testing, and packaging of GaN HEMTs tailored for radar and electronic warfare applications. With a solid foundation in circuit design and measurement validation, he brings a comprehensive approach to advancing high-performance RF and microwave systems.



Ahsan-Ullah Kashif received his MS degree in Material Physics and Nano Technologies and PhD degree in Semiconductor Physics from Linköping University, Linköping, Sweden, in 2005 and 2010, respectively. He has been working as a Senior Researcher at CESAT, Islamabad, and as an Adjunct Professor at the IIU, Islamabad, Pakistan. He has an enormous amount of experience in the field of RF communication, from RF device level

design to system level applications. His current research interests include design, development, and characterization of power amplifiers, receivers, and RF frontends for different communication bands.



Ekmel Ozbay received MS and PhD degrees from Stanford University, Stanford, CA, USA, in Electrical Engineering, in 1989 and 1992. He worked as a postdoc at Stanford University and later as a scientist at Iowa State University, Ames, IA, USA. He joined Bilkent University, Ankara, Turkey, in 1995, where he is currently a full professor in the Physics and Electrical and Electronics Engineering Departments. In 2003, he founded the Nanotechnology Research Center (NANOTAM),

Bilkent University, Ankara, Türkiye, where he leads a research group working on nanophotonics, nanoelectronics, nanometamaterials, and GaN-based devices. He is the 1997 recipient of the Adolph Lomb Medal of OSA and the 2005 European Union Descartes Science award. He worked as an editor for Optics Letters, PNFA, SPIE JNP, and IEEE JQE journals. He has published 600+ articles in SCI journals. His papers have received 34000+ citations with an h-index of 89. He is also the CEO of a spin-off company: AB-MicroNano Inc., which is founded to commercialize the technologies developed in NANOTAM.